Anomalous laser-induced ionization rates of molecules and rare-gas atoms

Jerry Ray Bettis
5701 Woodlake Drive, Stillwater, Oklahoma 74074, USA
(Received 5 October 2009; published 10 December 2009)

Electron tunnel ionization is considered as the mechanism for producing free electrons in gases under laser radiation. The Keldysh result and the Ammosov-Delone-Krainov (ADK) formulation are amended by considering the excess forces due to the interaction of the electric field of the laser with the electron cloud in a simple mass-on-a-spring approximation. The result of this excess force is a kinetic energy that is directed along the polarization vector of the laser field and an induced potential energy that are proposed as a determining factor in electron tunnel ionization. Relative ionization rates for various pairs of gases are calculated and compared with reported figures. Comparisons were made between several combinations of O_2, Xe, Ar, N_2, Cl_2, H_2, CO, Kr, NO, F_2, and D_2. Predicted ratios of ionization rates between pairs of gases are compared to ADK predictions. Apparently anomalous ionization rates of O_2, D_2, and H_2 are explained. A simple expression is developed that reveals why the ionization rate of Xe is about an order of magnitude larger than that of O_2 even though their ionization potentials are nearly identical; why CO is only about half that of Kr even though their ionization potentials are nearly the same; why the ratio of O_2 to O is about ten times larger than predicted by ADK; and why the ratio of NO to Xe is about an order of magnitude less than predicted by ADK.

DOI: 10.1103/PhysRevA.80.063420 PACS number(s): 33.80.Rv, 32.80.Rm, 34.50.Gb, 42.50.Hz

I. INTRODUCTION

Present multiphoton and electron tunnel ionization descriptions of laser-induced ionization in gases do not properly account for observed ionization rates [1–10]. The Keldysh [11] and Ammosov-Delone-Krainov (ADK) [12] models for electron tunnel ionization predict that O_2 and Xe should have the same ionization rate under strong optical electric fields because their ionization potentials are very nearly the same. The experiments of Talebpour *et al.* [1] revealed an order of magnitude difference in the ionization rates for these two gases. This apparently anomalous result has led researchers to compare the ionization rates of other pairs of gases with nearly equal ionization potentials. It has also fueled concerted efforts to offer explanations for each apparently anomalous result. Among the processes considered were: dissociative recombination, other dissociation processes, Stark shift, the presence of any accidental electronic resonance in the molecule, and electron localization in diatomic molecules [2]; the two-center nature of the potential and orientation of the molecular axis with respect to the laser polarization [3]; electron screening due to multielectron motion [4]; bonding symmetry versus antibonding symmetry of the valance orbitals of homonuclear diatomic molecules [5]; length and velocity gauge formulations of the molecular strong-field approximation and the effects of nuclear motion [9]; and *S*-matrix formalism of conventional strong-field approximation supplemented by the standard linear combination of atomic orbitals and molecular orbitals utilized for approximate analytical reproduction of the two-centered wave function of an initial molecular bound state [10].

None of these proposed explanations of results that are at variance with the Keldysh [11] and ADK [12] formulations has proven satisfactory. In many instances one apparent anomaly is explained while another remains elusive. Most of the authors conclude that a correct explanation has not yet been given. Finally, although the work of Usachenko *et al.* [10] showed some promise, it appears to require a separate explanation for each comparison and as such must be regarded as somewhat less than desirable.

It would appear that a single explanation, however simple, might reduce the increasingly complicated reasons given for the observed ionization rate ratios. It is the purpose of this paper to suggest a single explanation for the observed ratios of ionization rates between several species. This is a very elementary treatment, which is described in order to seek a first-order explanation for the perceived discrepancies.

Electron tunnel ionization, taking into account the kinetic and potential energies temporarily gained by the bound electrons through their polarizabilities, offers an explanation of the Xe/O_2 anomaly that agrees with the observed results. It also correctly predicts the relative ionization rate ratios for 11 species considered. Making use of the polarizability was suggested by the observation [13,14] that optical materials with larger refractive indices damage at lower fluence levels under laser radiation than lower index materials. The fit of the model proposed here is better than the fit of the ADK model for every comparison between gases with similar ionization potentials except for the trivial cases of N_2 versus Ar and F_2 versus Ar in which both the ionization potential and the polarization were sensibly the same.

II. THEORY

The present work follows the lead of Gamow in which he treated alpha particles within a nucleus as classical motion and applied wave theory to calculate the tunneling probability [15,16]. For simplicity, the assumption is made that the optical electric field of the laser interacts with the neutral atom or molecule as if all of the induced motion were concentrated in a single active electron (SAE). This electron exists in a potential well whose depth is the first ionization potential, I_p. Upon application of an electric field, $E(t)$, a potential, $eE(t)x(t)$, is developed, where e is the electron

charge and $x(t)$ is the distance measured from the electron's equilibrium position. As has been done from Keldysh [11] onward, the potential barrier formed by the Coulomb field of the atom and the applied field of the laser can be approximated to first order by a triangular potential. We shall proceed by using a semiclassical approximation to describe the motion induced by the optical field on the SAE and calculate the probability for tunneling through this barrier. If the barrier is sufficiently wide, one is justified in using a semiclassical approach. Furthermore, for a wide barrier, there is very little leakage of electrons out of the atoms and the wave functions inside the atom will be nearly those of the undisturbed stationary states. This allows one to ignore the time dependence of the Schrödinger equation and apply the WKB approximation [17,18] to the spatial portion of the equation. For simplicity we will consider only spherically symmetric wave functions corresponding to emission of electrons with zero angular momentum. This allows the three-dimensional problem to be considered as a one-dimensional problem.

We assume that the SAE is in a stable circular orbit and that the optical field acts on it to drive it about its stationary orbital position. The electron then executes simple harmonic motion about its equilibrium position in the direction of the polarization of the applied field. This motion, of course, is the source of development of the refractive index in dense media under low applied fields. The contention is that even though the fields are strong enough to ionize individual atoms and molecules, they are still well below the internal fields of the atoms and, as such, may be considered as small perturbations. In fact, for Xe the instantaneous potential energy gained by the electron is less than 7% of the ionization potential under interaction with a laser flux of 1×10^{15} W/cm^2. The corresponding maximum displacement of the SAE is about 0.2 Å, which is roughly 20% or less of the radius of most atoms in this paper. A question arises about adiabaticity when discussing kinetic and potential energies gained by the SAE. Just as in ordinary light passing through substances this motion of the SAE is merely a small oscillation about its equilibrium position, and there is no net energy exchange. Thus, this will be considered an adiabatic process. Also note that no splitting of energy levels is envisioned, thus this does not involve the Stark effect.

As will be shown, the present treatment results in an equation that may answer some of the apparently anomalous results when comparing single ionization rates for two neutral species that have nearly the same ionization potential but different polarizability.

Consider the motion of the SAE in the potential energy shown in Fig. 1 or its equivalent in Fig. 2.

For convenience of calculation and with no loss of generality, the zero point of the potential energy is set at the bottom of this total potential well [19]. The ionization potential, I_p, is then positive and the applied field, E, creates the portion of the potential, $I_p - E_{\{pot\}0} - eEx$, which separates region II from region III. These diagrams are a snap shot in time that changes as the laser cycle proceeds. In a simple mass-on-a-spring approximation the equation for the induced motion of the SAE is

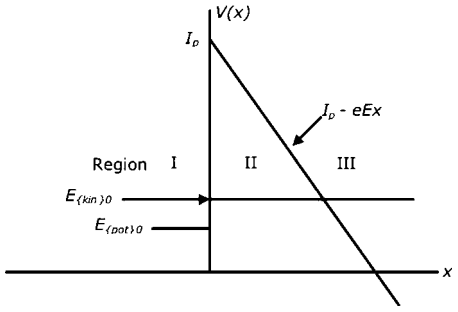

FIG. 1. Approximate potential barrier encountered by driven electron. $E_{\{pot\}0}$ is the potential energy gained by the SAE against the Coulomb restraining force at any time during the laser cycle and $E_{\{kin\}0}$ is the kinetic energy gained at the same time during the cycle and is shown additive to the $E_{\{pot\}0}$. The Coulomb potential is idealized as a rectangular potential with the zero taken at the bottom.

$$m\ddot{x} + m\gamma\dot{x} + kx = eEe^{i\omega_\ell t}, \tag{1}$$

where m is the mass of the electron, x is the induced displacement, γ is an effective damping coefficient, e is the electron charge, ω_ℓ is the laser frequency, and $k/m = \omega_0^2$ is the natural frequency of oscillation. Because the displacement oscillates at the driving frequency, $x(t) = xe^{i\omega_\ell t}$, one obtains a simplified equation of motion:

$$x(t) = \frac{e/m}{-\omega_l^2 + i\gamma\omega_l + \omega_0^2} E(t). \tag{2}$$

Clausius and Mosotti [20,21] showed that this is equivalent to

$$x(t) = \varepsilon_0 \alpha E(t)/e, \tag{3}$$

where ε_0 is the free-space permittivity and α is the polarizability.

Letting $E(t) = E\sin(\omega_\ell t)$, the induced kinetic energy is

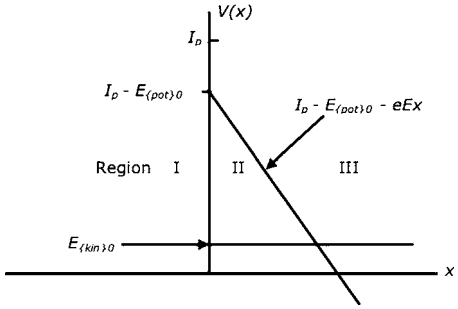

FIG. 2. Mathematically equivalent problem. For ease of calculation the Coulomb potential and the potential energy induced against the restraining force on the SAE are combined to more clearly reveal the elementary case of an electron with a known kinetic energy approaching a potential barrier. Here the induced kinetic energy of the electron is shown above the bottom of the total potential energy well, i.e., the difference between the ionization potential and the induced potential energy of the SAE.

$$E_{\{\mathrm{kin}\}} = 1/2m(\dot{x})^2 = 1/2m[\varepsilon_0 \alpha \omega_\ell E \cos(\omega_\ell t)/e]^2. \quad (4)$$

The potential energy gained by a mass-on-a-spring system with spring constant k is

$$E_{\{\mathrm{pot}\}} = 1/2kx^2. \quad (5)$$

For $\omega_\ell \ll \omega_0$, Eq. (2) can be approximated as

$$x(t) \cong \frac{(e/m)E(t)}{\omega_0^2} = \frac{(e/m)E(t)}{k/m}. \quad (6)$$

Using Eq. (3) to solve for the spring constant, k, yields

$$k \cong \frac{e^2}{\varepsilon_0 \alpha}. \quad (7)$$

Then the induced potential energy becomes

$$E_{\{\mathrm{pot}\}}(t) = 1/2k[x(t)]^2 = 1/2\frac{e^2}{\varepsilon_0 \alpha}[x(t)]^2. \quad (8)$$

With these expressions for the kinetic and potential energies associated with the motion one can write the wave function associated with the induced motion in region I as [19]

$$\psi_{\mathrm{I}}(x) = Ae^{ik_0 x} + Be^{-ik_0 x}, \quad (9)$$

where, $k_0 = mv/\hbar$, with v given in Eq. (4).

Anticipating use of the WKB approximation we write the wave function in region II as

$$\psi_{\mathrm{II}}(x) = \frac{C}{\sqrt{\kappa(x)}}\exp\left[-\int_0^x \kappa(x)dx\right] + \frac{D}{\sqrt{\kappa(x)}}\exp\left[\int_0^x \kappa(x)dx\right], \quad (10)$$

where

$$\kappa(x) = \sqrt{\frac{2m}{\hbar^2}((I_p - E_{\{\mathrm{pot}\}0} - eEx) - E_{\{\mathrm{kin}\}0})} = \sqrt{\frac{2m}{\hbar^2}[(I_p - eEx) - \mathcal{E}_0]}. \quad (11)$$

Here the total energy of the electron, $\mathcal{E}_0 = \mathcal{E}_0(t)$, is the sum of the kinetic and potential energies of the induced motion, $\mathcal{E}_0(t) = E_{\{\mathrm{kin}\}0}(t) + E_{\{\mathrm{pot}\}0}(t)$, with $E_{\{\mathrm{pot}\}0}(t)$ and $E_{\{\mathrm{kin}\}0}(t)$ calculated from Eqs. (4) and (8).

Finally, in region III the wave function is

$$\psi_{\mathrm{III}}(x) = \frac{A_1}{\sqrt{k_1(x)}}\exp\left[i\int_\ell^x k_1(x)dx\right] + \frac{B_1}{\sqrt{k_1(x)}}\exp\left[-i\int_\ell^x k_1(x)dx\right]. \quad (12)$$

The B_1 term is zero as we assume there are no electrons approaching from the right. To determine k_1, we note that the asymptotic wave function must be that of an electron accelerating to the right under the influence of the electric field. Thus, $k_1 = \frac{\sqrt{2m}}{\hbar}\sqrt{eE(x-\ell)}$, where ℓ, the turning point, is the width of the forbidden region. The probability density, $|\psi_{\mathrm{III}}(x)|^2$, is therefore a maximum at the turning point where the propagation number is zero and decreases as the electron is driven away from the atom or molecule. One cannot equate the internal and external probability current densities in order to find the transmission coefficient because under the influence of the applied field the probability current density is not conserved. The task, then, is to determine the ratios of the ionization probability densities of two species at the same applied electric field. We can arbitrarily assign k_1 for a pair of species because at constant electric field they will cancel out when forming the ratio of the probabilities for ionization.

To proceed we require continuity of the wave functions at the boundary between regions I and II:

$$\psi_{\mathrm{I}}(0) = A + B = \frac{1}{\sqrt{\kappa(0)}}(C + D) = \psi_{\mathrm{II}}(0), \quad (13)$$

and the continuity of the derivatives at the boundary:

$$\psi_{\mathrm{I}}'(0) = ik_0(A - B) = \sqrt{\kappa(0)}(-C + D) = \psi_{\mathrm{II}}'(0). \quad (14)$$

Here we have performed the derivative on the right side of Eq. (10) in the rapidly changing exponential only and neglected the relatively minor effect of $\kappa'(x)$ on the amplitude. Here the prime denotes differentiation with respect to x.

Solving these two Eqs. (13) and (14) we find

$$C = \frac{2Ak_0\sqrt{\kappa(0)}}{k_0 + i\kappa(0)}, \quad (15)$$

and to keep the solutions finite the value of D is set to zero.

To match wave functions at the boundary of regions II and III we use the WKB connection formulas suitable for a barrier to the left of the turning point, $x = \ell$ [16]. First we must write the wave function in region II appropriate to the turning point, $x = \ell$.

We note that

$$\exp\left[\int_0^x f(x)\right] = \exp\left[\int_0^\ell f(x)\right]\exp\left[\int_\ell^x f(x)\right] \quad (16)$$

and designate $\exp[\int_0^\ell f(x)] = e^\sigma$ so that

$$\psi_{\mathrm{II}}(x) = \frac{Ce^{-\sigma}}{\sqrt{\kappa(x)}}\exp\left[-\int_\ell^x \sqrt{\frac{2m}{\hbar^2}(I_p - \mathcal{E} - eEx)}dx\right]. \quad (17)$$

Then from the connection formula [14,15]

$$Ce^{-\sigma} = \theta^* A_1, \quad (18)$$

where

$$\theta = e^{i\pi/4}. \quad (19)$$

From Eqs. (15), (18), and (19) we obtain

$$Ce^{-\sigma} = \frac{2Ak_0\sqrt{\kappa(0)}}{k_0 + i\kappa(0)}e^{-\sigma} = \theta^* A_1 \quad (20)$$

and form the ratio of the ionization probability density to the incident probability density

$$\left|\frac{\Psi_{\mathrm{III}}}{\Psi_{\mathrm{I}}}\right|^2 = \left|\frac{A_1/\sqrt{k_1}}{A}\right|^2 = \frac{4k_0^2\kappa(0)e^{-2\sigma}}{k_1[k_0^2+\kappa(0)^2]}. \quad (21)$$

This is the ratio of the ionization probability density to the incident probability density, which we are seeking.

To complete the calculation of the probability we evaluate the exponential factor, $e^{-2\sigma}$.

From Eq. (16)

$$\sigma = \int_0^\ell \sqrt{\frac{2m}{\hbar^2}(I_p - \mathcal{E} - eEx)}dx$$

$$= -\frac{2\sqrt{2m}}{3\hbar eE}[I_p - E_{\{\mathrm{kin}\}0}(t) - E_{\{\mathrm{pot}\}0}(t) - eEx]^{3/2}\Big|_0^\ell, \quad (22)$$

which, for $I_p - eE\ell = E_{\{\mathrm{kin}\}0}(t) + E_{\{\mathrm{pot}\}0}(t)$ gives

$$\sigma = \frac{2\sqrt{2m}}{3\hbar eE}[I_p - E_{\{\mathrm{kin}\}0}(t) - E_{\{\mathrm{pot}\}0}(t)]^{3/2}. \quad (23)$$

Finally, the probability of ionization per approach is

$$P_{\mathrm{I}} = \frac{4E_{\{\mathrm{kin}\}0}(t)\sqrt{[I_p - E_{\{\mathrm{kin}\}0}(t) - E_{\{\mathrm{pot}\}0}(t)]}}{\sqrt{eE(x-\ell)}[I_p - E_{\{\mathrm{pot}\}0}(t)]}$$
$$\times \exp\left\{\frac{-4\sqrt{2m}}{3\hbar eE(t)}[I_p - E_{\{\mathrm{kin}\}0}(t) - E_{\{\mathrm{pot}\}0}(t)]^{3/2}\right\}. \quad (24)$$

To obtain predictions based on this expression we numerically integrate to determine the average probability over a period of the laser radiation.

For single ionization with magnetic quantum number of zero and unity angular momentum quantum number, the kernel of the exponential in Eq. (24) is the same as the ADK expression with just the addition of the potential and kinetic energies of the bound electron. The major difference in the expressions is the inclusion of the $E_{\{\mathrm{kin}\}}$ and $E_{\{\mathrm{pot}\}}$ of the induced motion in Eq. (24). This has the effect of explaining why two species with very similar ionization potentials can have large differences in ionization rates. Equation (24) will be used to compare ionization rate ratios between two atoms or molecules with similar ionization potentials.

III. RESULTS

In order to tabulate results from Eq. (24) the material properties of ionization potential and polarizability were input for the 16 gases seen in Table I. Ratios of ionization rates were then calculated for various pairs of gases in order to compare the present treatment with experimental results. Just the ratios will be compared because as pointed out by Wells *et al.* [8] the individual ionization rates vary by up to eight orders of magnitude over the laser intensity range of interest, whereas the ionization rate ratios typically differ by less than an order of magnitude over the same range.

In each of the graphs in Fig. 3 the solid line is the ionization rate ratio predicted by Eq. (24) of this work and the dashed line is the prediction of the ADK model. The predictions are compared to various experiments. As can be seen from the solid line in Fig. 3(a), the calculated ratio for Xe/O_2 using Eq. (24) varies from 6 to 9 in the range of $I(\mathrm{W/cm^2})$ from 2×10^{13} to 8×10^{14}. This graph compares favorably with the data collected by Gibson [2], DeWitt [7], and Talebpour [1]. The DeWitt data are perhaps the most reliable because both species were irradiated simultaneously to avoid extreme difficulties inherent in replicating experimental setup between the comparison gases. The rate ratio predicted by the ADK formula is, as is to be expected, nearly constant at unity. The major factor in this apparent anomaly is the larger polarizability of Xe (4.04 $\mathrm{Å}^3$) as compared to O_2 (1.56 $\mathrm{Å}^3$).

TABLE I. Relevant parameters for a number of gases [22]. Comparisons with experimental results will be made for all of these except He, Ne, CO_2, and CH_4.

Species	Ionization potential (eV)	Polarizability ($\mathrm{Å}^3$)
Ar	15.7596	1.66
CH_4	12.61	2.45
Cl_2	11.48	1.83
CO	14.014	1.95
CO_2	13.78	2.51
D_2	15.467	0.783
F_2	15.697	1.38
H_2	15.43	0.787
He	25.5874	0.208
Kr	13.997	2.48
N_2	15.581	1.71
Ne	21.5645	0.381
NO	9.264	1.698
O	13.618	0.802
O_2	12.07	1.56
Xe	12.1298	4.04

A second observation from Fig. 3(b) is that D_2, with an ionization potential of 15.467 eV and a polarizability of 0.783 $\mathrm{Å}^3$, is predicted by Eq. (24) to have an ionization rate of 25–50 % of that of Ar (15.7596 eV and 1.66 $\mathrm{Å}^3$). From an ionization potential standpoint these gases should have nearly identical ionization rates under the influence of identical strong laser fields. The ratio predicted by Eq. (24) compares favorably with the experimental data of Talebpour *et al.* [3] and Wells *et al.* [8] and is about six times larger than the ADK prediction. Although Benis *et al.* [6] state that the ionization rate of deuterium is suppressed compared to argon, this is not the case. Deuterium does have a lower ionization rate than argon but the reason, if Eq. (24) is correct, is that the polarizability of D_2 is a factor of about two lower than that of Ar. A comparison of Ar vs H_2 with available data [10] produced similar results as would be expected from the similarity of the two forms of hydrogen with the H_2 values (15.43 eV and 0.787 $\mathrm{Å}^3$) nearly those of D_2.

In Fig. 3(c) the rate ratios of Ar and F_2 are compared. Because Ar (15.7596 eV and 1.66 $\mathrm{Å}^3$) and F_2 (15.697 eV and 1.38 $\mathrm{Å}^3$) have very similar ionization potentials and po-

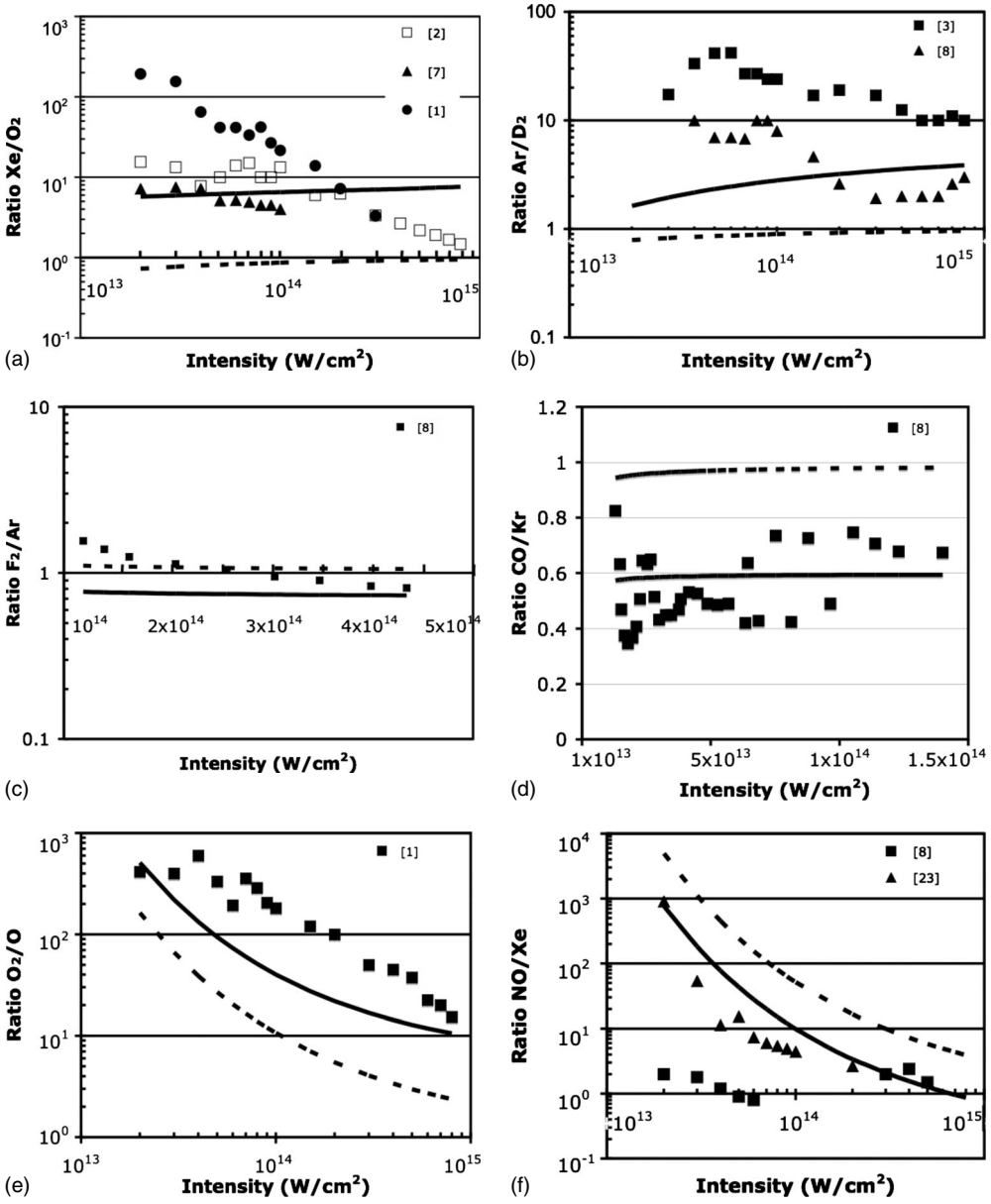

FIG. 3. Comparison of predictions of Eq. (24) and ADK with various pairs of atoms and molecules. Equation (24) provides a better fit for all except the trivial case of F_2 vs Ar for which the ionization potentials and polarizabilities are nearly the same. Equation (24) is solid and ADK is dashed line. Bracketed numbers refer to the listed references.

larizabilities one would expect them to have similar ionization rates. In fact, the slightly deeper potential well of Ar is offset by its slightly higher polarizability when compared to F_2, making their ionization rates very close to each other. In this case, the ADK results are closer to the experimental results than the present treatment. This result would seem to argue against the interference model [5], which predicted that F_2 would have an ionization rate nearly two orders of magnitude lower than Ar.

The case for CO (14.014 eV and 1.95 Å^3) versus Kr (13.997 eV and 2.48 Å^3) is instructive. Solely on the basis of ionization potential these two should have the same ionization rates. However, the polarizability of CO is only about 80% of that of Kr, which gives CO about 60% of the ionization rate of Kr as predicted by Eq. (24) and shown in the experimental results in Fig. 3(d).

Of interest is the ratio of the ionization rates of molecular versus atomic oxygen. The larger ionization potential of O (13.618 eV) compared to O_2 (12.07 eV) leads the ADK model to correctly predict a large O_2/O ratio. However, as can be seen in Fig. 3(e) the predicted ratio is about a factor of eight less than the measured value. An important consideration is the polarizability of O versus O_2, which is about a factor of two lower, 0.802 Å^3 for O compared to 1.56 Å^3 for O_2. This increased interaction in O_2 leads to a much larger ionization rate when compared to O and further increases the predicted ratio. As a result, the present treatment according to Eq. (24) provides a better fit to the data.

Figure 3(f) compares the ionization rates of NO to Xe. The data taken by Wells *et al.* [8] used a 1365 nm laser for the lower intensity values and a 790 nm laser for the higher intensities. It is unclear why the 1365 nm ratios are so much

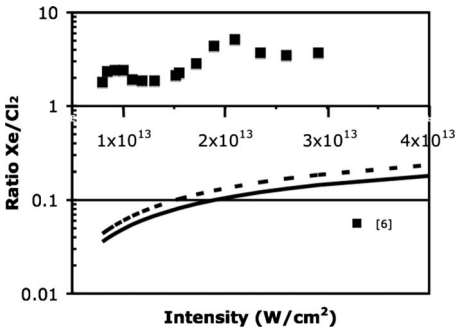

FIG. 4. Both ADK and the present work fail to predict the observed rate ratios of Xe vs Cl_2. Solid line, Eq. (24); dashed line, ADK.

lower than predicted by both Eq. (24) and the ADK model. The data by Walsh *et al.* [23] was shifted on the vertical axis to compare with their theory, so there is no absolute basis on which to compare the rate ratios. However, by anchoring the Walsh data to the Wells data at the higher intensities, it is possible to form ratios of NO to Xe for the entire range of interest. In fact, the results here have been shifted by about a factor of two on the vertical axis to provide a best fit to the present treatment. Both the present treatment and the ADK formulation predict that NO, with its 9.264 eV ionization potential will have a much higher ionization rate than Xe, with its 12.13 eV ionization potential. However, the larger polarizability of Xe compared to NO (4.04 $Å^3$ vs 1.698 $Å^3$) partially compensates for this. As can be seen in Fig. 3(f), Eq. (24) predicts a rate ratio about a factor of eight lower than ADK does.

The results of a comparison by Benis [6] of Xe (12.1298 eV and 4.04 $Å^3$) vs Cl_2 (11.48 eV and 4.71 $Å^3$) are shown in Fig. 4. Clearly, both the ADK model and Eq. (24) predict that Xe will have a lower ionization rate than Cl_2. This is due to both the smaller ionization potential and larger polarizability of Cl_2. The author was unable to locate an experimental value for the polarizability of Cl_2 and the value here reflects a calculation from [22]. The predicted results disagree with experiment and there is presently no explanation for this.

The author was unable to locate experimental results involving methane. However, such data could prove to be a critical test of the present theory. The ionization potential and polarizability of CH_4 (12.61 eV and 2.45 $Å^3$) places it squarely in the middle of the predicted ionization rates of O_2 and Xe. If the ionization rate of CH_4 were to fall within values predicted by the current Eq. (24), this would extend the present theory further into polyatomic molecules. Based on the properties of CH_4 (12.61 eV and 2.45 $Å^3$) and O_2 (12.07 eV and 1.56 $Å^3$), one would conclude from the ADK formulation that O_2 would have a higher ionization rate. However, the larger molecular polarizability of CH_4 leads Eq. (24) to predict a higher rate for CH_4 than O_2. In fact, the rate ratio from Eq. (24) is larger than the ADK rate ratio by factors from 2.6 to about 2.9 over the fluence range of interest here.

Both the ADK model and the present work closely predict the experimentally determined ratios for CO_2 vs CO and N_2 vs Ar. The data for CO_2 vs CO are again found in the 10.6 μm work of Walsh *et al.* [23], thus there is not an absolute basis for forming the ratios. However, without shifting the vertical axes of their data, the fit of both ADK and Eq. (24) are within expectations. As can be seen from Table I, CO_2 (13.78 eV and 2.51 $Å^3$) with smaller ionization potential and larger polarizability than CO (14.014 eV and 1.95 $Å^3$) is expected to have a higher ionization rate, a fact borne out by the unshifted Walsh data.

In the case of N_2 (14.014 eV and 1.95 $Å^3$) vs Ar (15.7596 eV and 1.66 $Å^3$), the data varies from $0.5 < N_2/Ar < 1.9$ [2,7], with both ADK and the present Eq. (24) predicting ratios from 1.3 to 2.08 for the intensity range of interest. The predictions closely follow the DeWitt *et al.* [7] data and do not show evidence of suppression.

IV. SUMMARY

The model considered here depends on material properties such as polarizability and ionization potential as well as laser pulse duration and laser frequency. Treating atoms and molecules the same is certainly not the usual practice. However, the close fit of the developed equation to relative rates of ionization in diatomic and even triatomic molecules may be an indication that molecular structure plays a secondary role in the ionization process and that the interaction of the SAE with the laser field is the first-order effect. The probability for electron tunnel ionization was calculated based on kinetic and potential energy induced in the bound electrons in each laser cycle. A predictive model of laser-induced gas ionization was developed. Strong-field ionization rates predicted by the model agree substantially with measured rates, thereby suggesting an explanation for the perceived anomalously low rate of O_2 as compared to Xe; the suppressed ionization rates of D_2 compared with Ar; the reason D_2 is suppressed and F_2 is not; the supposed suppression of O_2 rates and the absence of suppressed rates in N_2; and why the rate of CO is only about half that of Kr. Left unexplained is the low ionization rate of Cl_2 when compared to Xe. Note that in every case where a species is suspected of having suppressed ionization rate, the polarizability—and therefore its ability to respond to the laser field—is decidedly lower than the companion species.

[1] A. Talebpour, C.-Y. Chien, and S. L. Chin, J. Phys. B **29**, L677 (1996).
[2] C. Guo, M. Li, J. P. Nibarger, and G. N. Gibson, Phys. Rev. A **58**, R4271 (1998).
[3] A. Talebpour, S. Larochelle, and S. L. Chin, J. Phys. B **31**, L49 (1998).
[4] C. Guo, Phys. Rev. Lett. **85**, 2276 (2000).
[5] J. Muth-Böhm, A. Becker, and F. H. M. Faisal, Phys. Rev. Lett. **85**, 2280 (2000).
[6] E. P. Benis, J. F. Xia, X. M. Tong, M. Faheem, M. Zamkov, B. Shan, P. Richard, and Z. Chang, Phys. Rev. A **70**, 025401 (2004).
[7] M. J. DeWitt, E. Wells, and R. R. Jones, Phys. Rev. Lett. **87**, 153001 (2001).
[8] E. Wells, M. J. DeWitt, and R. R. Jones, Phys. Rev. A **66**, 013409 (2002).
[9] T. K. Kjeldsen and L. B. Madsen, Phys. Rev. A **71**, 023411 (2005).
[10] V. I. Usachenko and Shih-I Chu, Phys. Rev. A **71**, 063410 (2005).
[11] L. V. Keldysh, Sov. Phys. JETP **20**, 1307 (1965).
[12] M. V. Ammosov, N. B. Delone, and V. P. Krainov, Sov. Phys. JETP **64**, 1191 (1986).
[13] J. R. Bettis, A. H. Guenther, and R. A. House II, Opt. Lett. **4**, 256 (1979).
[14] J. R. Bettis, Appl. Opt. **31**, 3448 (1992).
[15] See, for example, R. B. Leighton, *Principles of Modern Physics* (McGraw-Hill, New York, 1959), p. 524.
[16] D. Park, *Introduction to the Quantum Theory* (McGraw-Hill, New York, 1964), pp. 92 and 353–361.
[17] E. Merzbacher, *Quantum Mechanics* (Wiley & Sons, New York, 1970), p. 118.
[18] L. I. Schiff, *Quantum Mechanics* (McGraw-Hill, New York, 1955), p. 184.
[19] A. S. Davydov, *Quantum Mechanics* (Pergamon Press, Oxford, 1965), pp. 79–83.
[20] J. D. Jackson, *Classical Electrodynamics* (Wiley & Sons, New York, 1963), p. 119.
[21] R. P. Feynman, R. B. Leighton, and M. Sands, *The Feynman Lectures on Physics* (Addison-Wesley, Reading, MA, 1963), Vol. II, pp. 32–37.
[22] K. P. Huber and G. Herzberg, in *NIST ChemistryWebBook: NIST Standard Reference Database 69*, edited by P. J. Lindstrom and W. G. Mallard (National Institute of Standards and Technology, Gaithersburg, MD, 2001), http://webbook.nist.gov.
[23] T. D. G. Walsh, F. A. Ilkov, J. E. Decker, and S. L. Chin, J. Phys. B **27**, 3767 (1994).